THE CCFM EQUATION AND PREDICTIONS FOR HERA PHYSICS*

P.J. SUTTON

Department of Physics and Astronomy, University of Manchester
Brunswick Street, Manchester, M13 9PL, England

(Received March 23, 1996)

We solve a unified integral equation (the CCFM equation) for the gluon distribution of a proton in the small x regime. Here x is the longitudinal momentum fraction of a gluon probed at a scale Q. The equation generates a gluon with a steep $x^{-\lambda}$ behaviour, with $\lambda \sim 0.5$. We compare our solutions with, on the one hand, those that we obtain using the double-leading-logarithm approximation to Altarelli–Parisi evolution and, on the other hand, to those that we determine from the BFKL equation. We examine what the consequences of this gluon evolution are for the structure function, $F_2(x, Q^2)$, as measured by the HERA electron-proton collider. Following this we investigate the effect of imposing an additional kinematic constraint, $k_T^2 < q_T^2/z$, on the CCFM equation. In particular we examine its implications for $F_2(x, Q^2)$ as a function of Q^2, the charm component, $F_2^c(x, Q^2)$ and diffractive J/ψ photoproduction.

PACS numbers: 12.38.Lg, 12.38.Qk

1. Introduction

The reliable prediction of many QCD processes requires a thorough understanding of the behaviour of parton distributions. In order to achieve this it is necessary to resum the large logarithms which arise, not just from single, but from multigluon emissions to all orders in α_S. A typical contribution is shown in Fig. 1, where a gluon of low space-like virtuality evolves to higher virtuality and lower energy by the emission of another gluon. Such logarithms are traditionally summed by either the DGLAP equation [1]

---

* Presented at the Cracow Epiphany Conference on Proton Structure, Kraków, Poland, January 5–6, 1996.

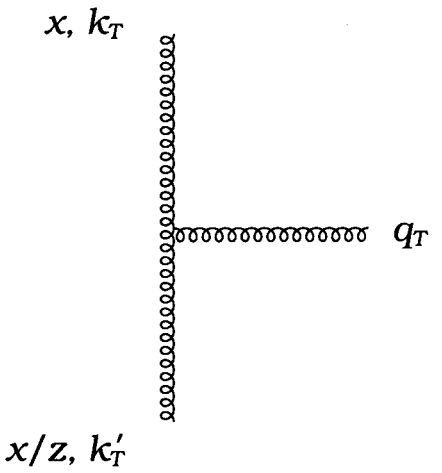

Fig. 1. Gluon emission which forms the basis of the evolution equation (3) for the unintegrated gluon distribution $F(x, k_T^2, Q^2)$. x and x/z are the longitudinal momentum fractions of the proton's momentum carried by the respective gluons. Throughout we use q_T and k_T to denote, respectively, the transverse momentum of an emitted gluon and of a gluon along the chain.

(Dokshitzer, Gribov, Lipatov, Altarelli and Parisi) or the BFKL equation [2] (Balitzkij, Fadin, Kuraev and Lipatov). These equations sum the $\alpha_s \log(Q^2)$ and $\alpha_s \log(1/x)$ terms respectively. They are therefore valid in quite separate regions of the (x, Q^2) kinematic region, depending on which set of logarithms is dominant. Recently, however, a theoretical framework which gives a unified treatment throughout the (x, Q^2) region has been provided by Catani, Ciafaloni, Fiorani and Marchesini [3, 4]. The resulting equation, which we shall call the CCFM equation, treats both the small and large x regions in a unified way. The equation is based on the coherent radiation of gluons, which leads to an angular ordering of the gluons along a chain of multiple emissions. The angular ordering introduces an additional scale (which turns out to be essentially the hard scale Q of the probe), which is needed to specify the maximum angle of gluon emission. The CCFM equation is thus defined in terms of a scale (Q) dependent *unintegrated* gluon density $F(x, k_T^2, Q^2)$, which specifies the chance of finding a gluon with longitudinal momentum fraction x and transverse momentum of magnitude k_T. The traditional *integrated* gluon density can be recovered via the relationship

$$xg(x, Q^2) = \int^{Q^2} dk_T^2 \, F(x, k_T^2, Q^2) \, . \tag{1}$$

At very small x the angular ordering does not provide any constraint on the transverse momenta along the chain and F becomes the Q-independent

gluon of the BFKL equation. At moderate x the angular ordering becomes an ordering in the gluon transverse momenta and the CCFM equation becomes equivalent to standard Altarelli–Parisi evolution.

In this contribution we examine the CCFM equation and its consequences for some physically observable quantities as measured by the HERA electron-proton collider. We begin in Section 2 with a brief review of the equation. This is followed in Section 3 with a comparison of a numerical solution of the CCFM equation with the corresponding DGLAP and BFKL solutions. In Section 4 we examine the consequences for the structure function, F_2, as measured at HERA. In section 5 we examine the effect of introducing an extra "consistency" constraint on the CCFM equation and in Section 6 we examine the effect of this constraint on predictions for $F_2(x, Q^2)$, its charm component, $F_2^c(x, Q^2)$ and the cross section for diffractive J/Ψ photoproduction. Section 7 contains our conclusions.

2. The CCFM equation

The CCFM equation is based on the summation of multigluon emissions which are coherent in the sense that there is angular ordering, $\theta_i > \theta_{i-1}$, along the chain, where θ_i is the angle that the i^{th} gluon makes to the original direction [3, 4]. Outside this region there is destructive interference such that the multigluon contributions vanish to leading order.

It is convenient to express the concept of angular ordering in terms of the various gluon momenta. Firstly it is helpful to introduce the rescaled transverse momenta

$$q \equiv \frac{q_T}{1-z} \approx \theta E', \quad q' \equiv \frac{q'_T}{1-z'} \approx \theta' E'', \tag{2}$$

where $1-z$ is the longitudinal momentum fraction of the gluon emitted at angle θ and E' is the energy component of the exchanged gluon with spacelike momentum $x'p$. Here we have used the small angle approximation, $\tan\theta \approx \theta$. The coherence constraint $\theta > \theta'$ therefore implies $q > z'q'$.

With the angular ordering constraint expressed as a theta function, the CCFM equation is given by

$$F(x, k_T^2, Q^2) = F^0(x, k_T^2, Q^2) + \int_x^1 dz \int \frac{d^2q}{\pi q^2} \Theta(Q - zq) \Delta_S(Q, zq) \tilde{P}(z, q, k_T) F\left(\frac{x}{z}, k_T'^2, q^2\right). \tag{3}$$

The inhomogeneous or "no-rung" contribution, F^0, may be regarded as the non-perturbative driving term. It should be noted that the variable k'_T is the magnitude of the vector sum $\boldsymbol{k_T} + (1-z)\boldsymbol{q}$ and, so, in principle, the angular integration in d^2q is non-trivial. The function $\tilde{P}$ is the gluon-gluon splitting function

$$\tilde{P} = \overline{\alpha}_S \left[\frac{1}{1-z} + \Delta_R \frac{1}{z} - 2 + z(1-z) \right], \tag{4}$$

where $\overline{\alpha}_S \equiv C_A \alpha_S/\pi = 3\alpha_S/\pi$. The multiplicative factors Δ_S and Δ_R are known as the Sudakov and Regge form factors. They arise from the resummation of the virtual corrections and cancel the singularities manifest as $z \to 1$ and $z \to 0$ respectively. Their explicit form can be found in, for example, Ref. [5].

3. Numerical solution of the CCFM equation

In this contribution we are interested in the CCFM equation at small x. In this region we may simplify the equation (3) as follows

$$F(x, k_T^2, Q^2) = F^0(x, k_T^2, Q^2) + \overline{\alpha}_S \int_x^1 \frac{dz}{z} \int \frac{d^2q}{\pi q^2} \Theta(Q - zq) \Delta_R(z, q, k_T) F\left(\frac{x}{z}, (\boldsymbol{k_T} + \boldsymbol{q})^2, q^2\right), \tag{5}$$

where we have set $\Delta_S = 1$ and retained only the $1/z$ term in the splitting function $\tilde{P}$. We have also approximated $(1-z)q$ by q in the argument k'_T of F. In this small x limit, the variable q reduces to the transverse momentum q_T of the emitted gluon, see Eq. (2). This simplified form of the CCFM equation is the one which we shall investigate. This requires us to make several choices. Firstly we need to specify the scale of the running coupling, α_s. We take this scale to be k_T^2 since this value is usually assumed for small x studies involving the BFKL equation. Secondly, we need to assume some form for the driving term, F^0. We would like to choose something simple, so we choose our F^0 such that it would generate a "flat" gluon, $xg \sim 3(1-x)^5$, in the absence of angular ordering and the Δ_R correction term. As F corresponds to the unintegrated gluon we also need to specify its initial k_T^2 dependence. We take an exponential form $\exp(-k_T^2/Q_0^2)$ with

Q_0^2 taken to be 1 GeV^2. The driving term is then given by

$$F^0(x,k_T,Q;\mu^2) = N\exp(-k_T^2/Q_0^2)\int_x^1 \frac{dz}{z}\Theta(Q-k_Tz)\Theta(Q^2-\mu^2)$$

$$\tilde{\Delta}_R(z,k_T,k_T;\mu^2)\frac{d[3(1-x/z)^5]}{d\log(z/x)}, \qquad (6)$$

where the normalization, N, is fixed to ensure that the gluon carries half of the momentum of the proton. For computational convenience we have introduced a resolution variable, μ^2, which will have the effect of providing a lower cut-off on the dq^2 integration in the CCFM equation (5). This parameter can, however, be chosen sufficiently small ($\mu^2 \sim 10^{-2}$) so that it does not affect the final result [5]. With these choices we solve (5) by iteration from the starting distribution (6). We restrict the iterative procedure to the domain $k_T^2, k_T'^2 > Q_0^2 = 1$ GeV^2. We also introduce an upper limit cut-off, Q_F^2, on the q^2 integrations which is in the region $10^4 - 10^5$ GeV^2, though the results are insensitive to variations around and above these values.

The calculation is now repeated using the double-leading-logarithm (DLL) approximation[1] in which we replace angular ordering, $\Theta(Q-zq)$, by ordering in transverse momenta, $\Theta(Q-q)$, and in which we set $\Delta_R = 1$. In this case the equation reduces to

$$F(x,k_T^2,Q^2) = F^0(x,k_T^2,Q^2) + \bar{\alpha}_S\int_x^1 \frac{dz}{z}\int \frac{d^2q}{\pi q^2}\Theta(Q-q)F(\frac{x}{z},k_T'^2,q^2)\,. \quad (7)$$

Fig. 2 shows our solution for both equations in terms of the integrated gluon distribution, $xg(x,Q^2)$ of (1) with lower limit Q_0^2. Remember that the gluon distribution is generated radiatively from an input which is "flat" at small x, and so the rapid rise of the CCFM gluon with decreasing x is generated by the CCFM equation. By contrast the dashed curves in Fig. 2 show the characteristic double-leading-logarithm (DLL) small x behaviour

$$xg(x,Q^2) \sim \exp\left[2\{\xi(Q^2,Q_0^2)\log(1/x)\}^{\frac{1}{2}}\right] \qquad (8)$$

appropriate to a "flat" input, that is $xg(x,Q_0^2) \to$ constant as $x \to 0$.

---

[1] This procedure only becomes equivalent to the conventional DLL approximation for $xg(x,Q^2)$ after we integrate over k_T.

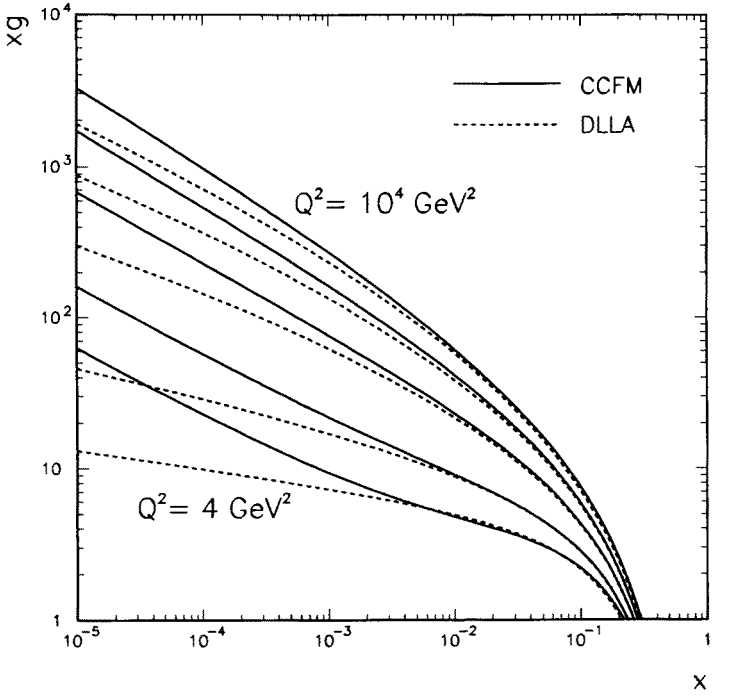

Fig. 2. The integrated gluon distribution xg versus x, obtained from both the CCFM (continuous curves) and the DLL (dashed curves) integral equations, for $Q^2 = 4, 10, 10^2, 10^3$ and 10^4 GeV^2. Recall that our solutions are obtained from a "flat" gluon input.

To quantify the increase in xg, we show in Fig. 3 the effective value of λ, defined by

$$xg(x, Q^2) = Ax^{-\lambda}. \tag{9}$$

For small x we see that the solutions converge to a typical $x^{-0.5}$ behaviour, approximately independent of Q^2, which, as we shall see below, is consistent with that obtained from the solution of the (leading $\log(1/x)$) BFKL equation. To be precise we solve the BFKL equation

$$F(x, k_T) = F^{0L}(x, k_T) + \overline{\alpha}_S(k_T^2) \int_x^1 \frac{dz}{z} \int_{Q_0^2}^{\infty} \frac{dk_T'^2}{k_T'^2} \times \left\{ \frac{k_T'^2 F(z, k_T') - k_T^2 F(z, k_T)}{|k_T'^2 - k_T^2|} + \frac{k_T^2 F(z, k_T)}{(4k_T'^4 + k_T^4)^{\frac{1}{2}}} \right\}, \tag{10}$$

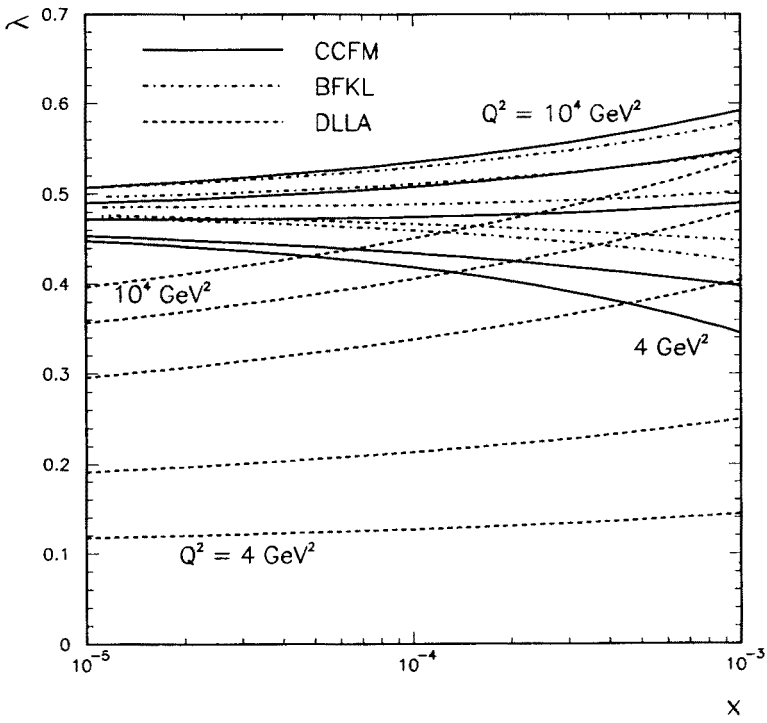

Fig. 3. The effective values of λ, defined by $xg = Ax^{-\lambda}$. The CCFM values (continuous curves) are compared with those obtained from the BFKL (dot-dashed curves) and DLL approximations (dashed curves). In each case we show curves corresponding to five different values of Q^2.

with the driving term

$$F^{0L}(x, k_T) = 3(1-x)^5 N \exp(-k_T^2/Q_0^2)\,. \tag{11}$$

The integration region is restricted to $k_T'^2 > Q_0^2 = 1$ GeV^2. Fig. 3 shows the resulting effective slopes $\lambda_{\mathbf{eff}}$. Since the solution, $F(x, k_T)$, of the BFKL equation is independent of Q, the Q^2 dependence observed for xg comes entirely from the k_T integration of (1). On the other hand the solution $F(x, k_T^2, Q^2)$ of the CCFM equation has an intrinsic Q dependence arising from angular-ordering, $\Theta(Q - qz)$. From Fig. 3 we note that the effective slopes, $\lambda_{\mathbf{eff}}$, of the integrated CCFM and BFKL gluons are remarkably

similar at small x. We conclude that the next-to-leading $\log(1/x)$ effects included in the CCFM formalism have a comparatively weak effect on the $x^{-\lambda}$ behaviour, although we note that the onset of the $x^{-\lambda}$ form is more delayed for the CCFM solution.

4. The structure function, F_2

The gluon distribution itself is, of course, not an observable. However, the behaviour of the gluon feeds through into physical quantities such as the structure functions. In deep inelastic scattering the virtual photon couples to the gluon via the $g \to q\bar{q}$ transition. We therefore calculate the structure function F_2 from the unintegrated gluon distribution F using the k_T-factorization theorem [6, 7]

$$F_2(x,Q^2) = \sum_q \int dk_T^2 \int_x^1 \frac{dx'}{x'} \int d^2\kappa F(x', k_T^2, \kappa^2) \times F_q^{\mathbf{box}}\left(\frac{x}{x'}, \vec{\kappa}_T, \vec{k}_T, Q^2, m_q\right) + F_2^S \,, \tag{12}$$

where $F_q^{\mathbf{box}}$ includes both the quark "box" and "crossed box" contributions which originate from virtual photon-virtual gluon $q\bar{q}$ production, that is from $\gamma g \to q\bar{q}$. The convolution is sketched in Fig. 4. For the u, d and s quark contributions we take the quark mass $m_q = 0$, while for the charm component we take $m_c = 1.5$ GeV. The explicit expressions for $F_q^{\mathbf{box}}$ including quark mass effects can be found[2] in Ref. [8]. The background contribution, F_2^S, behaves as $F_2^S \simeq F_2(x,Q^2)$ at large x, but is a slowly varying function of x and Q^2 at small x.

Before calculating F_2 there is an extra correction that we can apply to our gluon distribution to improve its Q^2 dependence. Recall that the small x approximation of the CCFM equation that we have used amounts to setting the Sudakov form factor $\Delta_S = 1$ and to approximating the gluon-gluon splitting function by its singular term as $z \to 0$, that is $P_{gg} \simeq 6/z$. We can, however, approximately account for the remaining finite terms in P_{gg} by multiplying the solution $F(x, k_T^2, Q^2)$ by the factor

$$\exp\left(-A \int^{Q^2} \bar{\alpha}_S(q^2) \frac{dq^2}{q^2}\right) , \tag{13}$$

[2] There is a typographical error in the expression for x' below Eq. (19) in Ref. [8]; the factor $\beta(1-\beta)$ should be in the denominator.

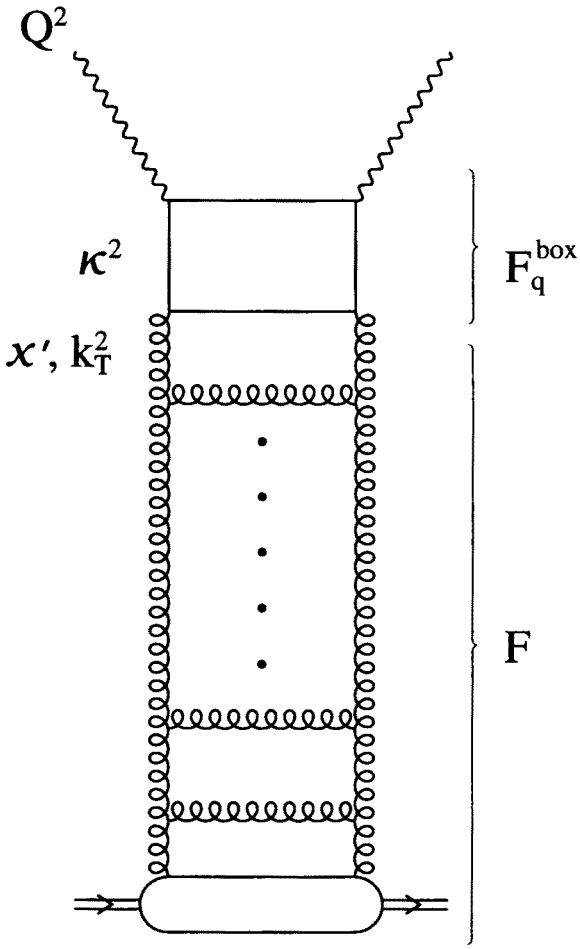

Fig. 4. Pictorial representation of the k_T factorization formula, that is of the convolution $F_2 = \sum_q F \otimes F_q^{\text{box}}$ of (12). $F(x', k_T^2, \kappa^2)$ is the unintegrated gluon distribution and $\sum_q F_q^{\text{box}}$ is the off-shell gluon structure function, which at lowest order is determined by the quark box (and "crossed box") contributions.

where A is defined by

$$\int_0^1 z^\omega P_{gg}(z)dz \simeq \frac{6}{\omega} - 6A\,. \tag{14}$$

That is $A = (33 + 2n_f)/36$, where the number of active flavours $n_f = 4$. With this factor (13) included we calculate F_2 using the formula (12).

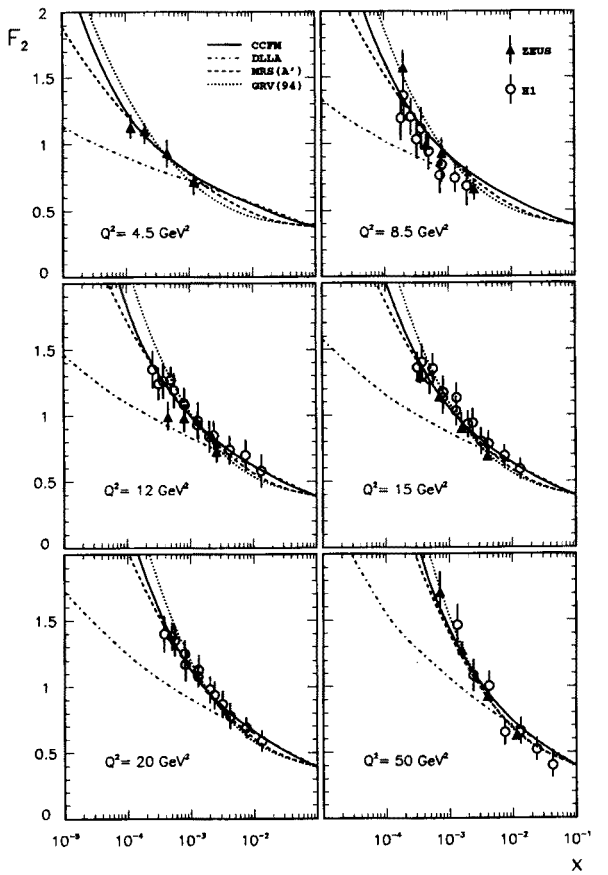

Fig. 5. A comparison of the HERA measurements of F_2 [9, 10] with the predictions obtained from the k_T-factorization formula (12) using for the unintegrated gluon distribution F the solutions of the CCFM equation (continuous curve), and the DLL-approximation (dot-dashed curve) of this equation. We also show the values of F_2 obtained from collinear factorization using the MRS(A′) [11, 12] and GRV [18] partons.

Fig. 5 compares the CCFM and DLLA predictions for F_2 with the recent HERA measurements [9, 10]. We use the k_T-factorization formula (12) with an infrared cut-off, $k_T^2 > k_0^2$. For the non-perturbative background contribution, F_2^S, we use the value of $F_2(x, Q^2)$ obtained from the MRS(A′) set of partons [11, 12] at $x = 0.1$, and extrapolate below 0.1 assuming the normal $x^{-0.08}$ "soft" behaviour.

From Fig. 5 we see that the CCFM and DLLA predictions coincide at large x, as indeed they should. The two schemes start to differ at small x

and Fig. 5 indicates the value of x at which the resummation effects become important. The rise of the gluon, and hence of F_2, is generated by the evolution equation and hence is within the domain of perturbative QCD. Of course, our prediction is not absolute. The normalisation depends on the choice of k_0^2, which delimits the infrared region, and also on the choice of the driving term and the lower limit of integration in (13). Here we take this to be $\overline{Q}_0^2 = 1$ GeV^2. Recall that the correction factor (13), and hence $\overline{Q}_0$, only occurs because we solve a simplified form of the CCFM equation appropriate to the small x region. In summary there is some freedom in the normalisation of F_2, though the prediction of the shape of the x dependence is characteristic of the CCFM equation. It is encouraging that the physically reasonable choice $k_0^2 = \overline{Q}_0^2 = 1$ GeV^2 gives a satisfactory description of the HERA data.

5. An additional constraint

There exists a kinematical constraint which is not included in the CCFM equation, but which is fairly easy to implement, it is [3, 13]

$$k_T^2 > z q_T^2 . \tag{15}$$

or, to be precise, it is actually [14]

$$q_T^2 < (1-z) k_T^2 / z . \tag{16}$$

The constraint[3] arises since, in the small z regime where the BFKL equation is valid, we require that the virtuality of the exchanged gluons arises mainly from the transverse, rather than the longitudinal, components of their momentum; that is

$$|k'|^2 \approx k_T'^2 . \tag{17}$$

There are also constraints from energy-momentum conservation [15] but these are not expected to be so important [14].

In the small z, large Q^2 regime the kinematic constraint $q_T^2 < (1-z)k_T^2/z$ is a stronger limitation than the angular ordering constraint $q^2 < Q^2/z^2$, and we anticipate that the CCFM solution $F(x, k_T^2, Q^2)$ will become independent of Q^2. In other words in this limit the kinematic constraint automatically embodies the angular ordering constraint [13] and since the former is independent of Q^2 the unintegrated gluon distribution F does not

[3] Throughout we call this a kinematic constraint although its origin is partly dynamical. The derivation of (16) can be found in Ref. [14].

depend on this variable either. However, as Q^2 decreases below k_T^2 the angular ordering constraint becomes stronger and F begins to decrease.

The effect of imposing this constraint on the gluon's effective slope, $\lambda_{\mathbf{eff}}$, is to make it smaller by about 0.1 [14]. However, of more immediate interest to us here is the effect it has on physical observables such as F_2. It is therefore to this subject that we now turn.

6. The impact on observables

Here we investigate the influence of the constraint X on several physical observables. These are the structure function, F_2, its charm component, F_2^c and the cross section for diffractive J/ψ photoproduction. Previously we examined the behaviour of F_2 versus x. Here we examine F_2 versus Q^2. This has the pleasant property that the slope, $\partial F_2/\partial \ln Q^2$, should be particularly insensitive to any ambiguities due to F_2^S. However, note that when Q^2 becomes large (beyond the range of the data that we consider here) some care is needed. The kinematic constraint is only applicable in the small x region and so the normalisation of the gluon is suspect at large x, particularly for large Q^2. We therefore, renormalise the solution of the CCFM equation with the kinematic constraint imposed so as to agree for $x > 0.1$ with the unmodified solution and its DLL approximation. In this way we allow for the small x approximation of the equation. The renormalisation only affects the solution for $Q^2 \gtrsim 20$ GeV^2. With this understood, we show in Fig. 6 the predictions for $F_2(x, Q^2)$ at small x together with the latest HERA measurements. Including the kinematic constraint (16) in the CCFM equation for the gluon $F(x, k_T^2, Q^2)$ has the effect of taking us from the dashed to the continuous curves in Fig. 6. The relevant comparison is the slope $(\partial F_2/\partial \ln Q^2)$ of the curves which is proportional to the gluon distribution. With the present experimental errors the comparison is inconclusive, but it is evident that, as the statistical and systematic errors are reduced, future measurements of $\partial F_2/\partial \ln Q^2$ will give insight into the properties of the gluon distribution $F(x, k_T^2, Q^2)$.

Recently the charm component of F_2 has been measured [16] at HERA in the small x region. These measurements of $F_2^c(x, Q^2)$ are shown in Fig. 7, together with earlier EMC values [17] at larger x. We compare these data with the charm component F_2^c determined from the gluon distribution, F, using the c quark contribution to the k_T-factorization formula (12). We show the values obtained by taking the mass of the charm quark to be $m_c = 1.4$ and 1.7 GeV. We also show predictions based on GRV [18] and MRS partons [12]. The first of these two is obtained from $\gamma g \to c\bar{c}$ at NLO [19] using massive charm quarks and the *integrated* (GRV) gluon distribution. In the MRS analyses [11, 12] the charm quark is treated as a parton. The charm

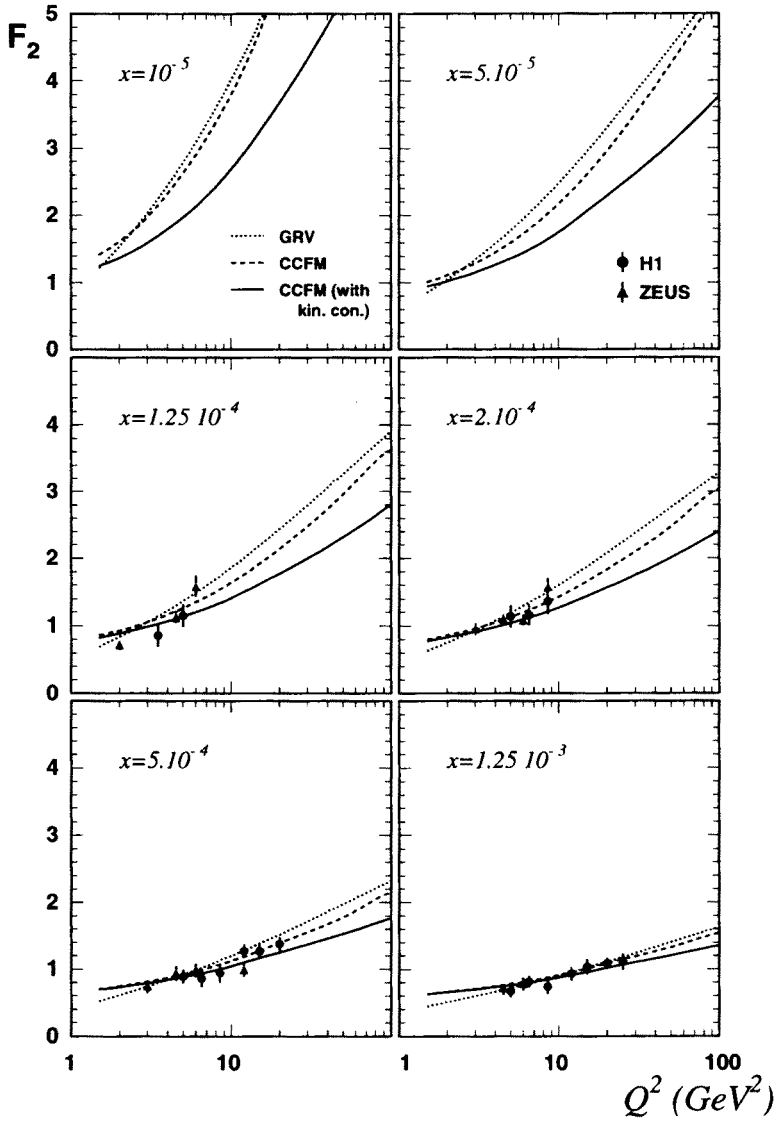

Fig. 6. Predictions of the proton structure function $F_2(x, Q^2)$ as a function of $\ln Q^2$, at fixed values of x, compared with recent measurements made by the experiments at HERA [9, 10]. The continuous and dashed curves are respectively the predictions obtained from the CCFM equation, via the k_T-factorization theorem, with and without the kinematic constraint (16) incorporated. The dotted curves are the predictions obtained from the GRV set of partons [18].

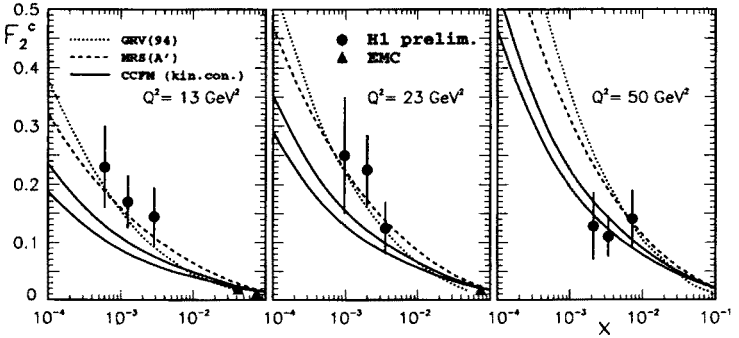

Fig. 7. Predictions for the charm component F_2^c of the proton structure function, F_2, compared to recent preliminary H1 measurements [16] and older EMC data [17]. The predictions were obtained by solving the CCFM equation (with kinematic constraint) for the unintegrated gluon and then using the k_T-factorization formula with $m_c = 1.4$ GeV (upper continuous curve) and $m_c = 1.7$ GeV (lower continuous curve) Also shown are the next-to-leading order predictions [19, 11] based on GRV [18] and MRS [12] partons.

distribution is assumed to be zero for $Q^2 < m^2$, while above this threshold ($Q^2 > m^2$) it is evolved assuming that $m_c = 0$. The value $m^2 = 2.7$ GeV^2 is determined by fitting to the EMC data [17] for F_2^c. Although the H1 small x data are preliminary, it is clear that an improved measurement of F_2^c will be valuable. At present there are indications that our k_T-factorization approach underestimates the H1 data at the lower Q^2 values; in fact the imposition of the kinematic constraint worsens our previous description of these data [20].

The final observable process that we study is high energy diffractive J/ψ photoproduction, $\gamma p \to J/\psi p$. Since this is essentially an elastic process, the cross section is dependent on the *square* of the unintegrated gluon distribution, $F(x, k_T^2, Q^2)$. The relevant values of x and Q^2 are $x = M_\psi^2/W^2$ and $\overline{Q}^2 \equiv M_\psi^2/4$, where M_ψ is the mass of the J/ψ meson and W is the γp centre-of-mass energy. The cross section is given by [21]

$$\sigma(\gamma p \to J/\psi p) = \frac{1}{b}\frac{d\sigma}{dt}(\gamma p \to J/\psi p)\Big|_0 = \frac{\pi^3 M_\psi^3 \alpha_S^2(\overline{Q}^2)\Gamma_{ee}}{3b\alpha} \times \left| \int \frac{dk_T^2}{k_T^2}\left(\frac{1}{M_\psi^2} - \frac{1}{M_\psi^2 + 4k_T^2}\right) F(x, k_T^2, \overline{Q}^2)\right|^2, \quad (18)$$

where Γ_{ee} is the leptonic width describing the $J/\psi \to e^+e^-$ decay, α is the

QED coupling, and b is the slope parameter of the differential cross section, $d\sigma/dt = A\exp(-b|t|)$. We take the experimental value $b = 4.5$ GeV^{-2}. We include the effects of $c\bar{c}$ rescattering and the small contribution of the real part of the amplitude as described in Ref. [21]. It was noted in Ref. [21] that the effects of Fermi motion of the c and $\bar{c}$ quarks in the J/ψ lead to a sizeable ($\pm 30\%$) uncertainty in the normalization of the perturbative QCD prediction of the photoproduction cross section, but that the "shape" of the W (or x) dependence is unaffected.

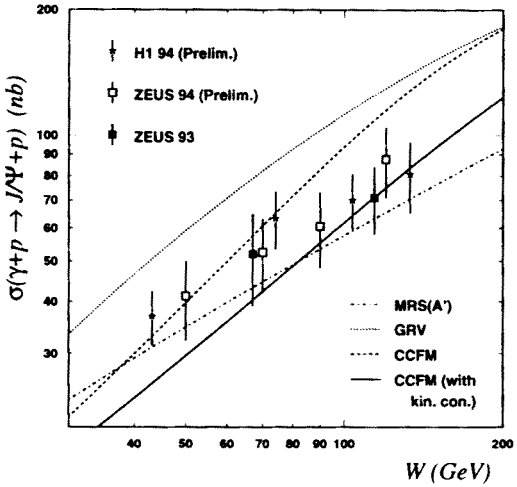

Fig. 8. The measurements [22] of the cross section for diffractive J/ψ photoproduction compared with the perturbative QCD description based on the unintegrated gluon distribution obtained by solving the CCFM equation with (continuous curve) and without (dashed curve) the kinematic constraint (16) included. The dotted and dash-dotted curves are the predictions obtained from the GRV and MRS(A′) set of partons [18, 12], calculated as in Ref. [21].

The predictions for diffractive J/ψ photoproduction are compared with recent HERA data in Fig. 8. At present the data extend up to energy $W \simeq 140$ GeV, that is down to $x \simeq 5 \times 10^{-4}$. The prediction in the absence of the kinematic constraint (the dashed curve) implies that the gluon increases too fast with decreasing x. On the other hand if the kinematic constraint is incorporated in the CCFM equation, then the continuous curve is obtained and the description is improved.

For completeness we also show in Fig. 8 the description of the J/ψ data calculated from two recent sets of partons (GRV [18] and MRS(A′) [12]) as described in Ref. [21]. Neither parton set incorporates $\ln(1/x)$ resummation effects. The J/ψ data appear to favour the phenomenological gluon distribution of the latter set of partons.

5. Conclusions

We have solved a unified equation for the unintegrated gluon distribution which incorporates BFKL dynamics at small x and Altarelli–Parisi evolution at larger x. We called it the CCFM equation after its originators — Catani, Ciafaloni, Fiorani and Marchesini. Starting from a driving term based on a "flat" $3(1-x)^5$ gluon with a narrow k_T distribution, $\exp(-k_T^2/Q_0^2)$, we used an iterative procedure to find the x dependence of the gluon.

We concentrated on the behaviour of the gluon in the small x regime. The key ingredients of the CCFM equation are the angular-ordering of gluon emissions and the presence of a Regge form factor. We found that the CCFM equation generates a gluon $F(x, k_T, Q)$ with a singular $x^{-\lambda}$ behaviour, with $\lambda \simeq 0.5$ The angular-ordering introduces a dependence of the unintegrated gluon on the scale Q, especially at the lower values of Q^2.

We compared our CCFM solutions with the conventional DLL approximation in which angular-ordering is replaced by strong-ordering in the gluon transverse momenta and in which the Regge form factor is omitted, $\Delta_R = 1$. The gluon was then found to be much less steep with decreasing x The DLL approximation starts to differ from the CCFM results in the region $x \lesssim 10^{-2}$. We also compared the CCFM solutions with the solutions of the BFKL approximation. Fig. 3 quantifies the $x^{-\lambda}$ agreement between the unified CCFM solution and the approximate BFKL solution. The agreement is remarkably good at small x, especially at the larger values of Q^2. Both the CCFM and BFKL solutions have a behaviour $xg \sim x^{-\lambda}$ at small x, where the value of λ is in the region of 0.5 with only a modest dependence on Q^2, in contrast to the dependence of λ on the evolution length for the DLL approximation.

We next examined what such a gluon distribution predicts for the structure function, F_2. We found reasonable agreement with the HERA data, but clearly this does not imply angular ordering effects have been firmly established. GLAP and BFKL evolution can give an equally good description. There are two characteristic features of the gluon distribution $F(x, k_T^2, \overline{Q}^2)$ obtained from an evolution equation which includes a resummation of $\ln(1/x)$ terms. These are a steep rise of f with decreasing x which is accompanied by a diffusion in $\ln k_T^2$. F_2 measures only the rise. A distinctive test will involve both features. For this we need to explore final state processes such as deep inelastic events containing an identified energetic forward jet. Here we have focused on F_2 and obtained predictions based on angular-ordered evolution which embodies both BFKL and GLAP resummations.

We have investigated the effect of imposing an extra constraint $\Theta(k_T^2/q_T^2 - z)$ on the evolution equation. This is needed to ensure that the virtuality of the gluons along the chain is controlled by the transverse momenta, that is $|k^2| \sim k_T^2$. For running α_S we solved the CCFM equation numerically and obtained the gluon distribution $F(x, k_T^2, Q^2)$ with the kinematic constraint imposed. In this case the constraint has the effect of reducing $\lambda_{\mathbf{eff}}$ by about 0.1.

In Section 6 we studied the impact of imposing the kinematic constraint on the description of three observables which are sensitive to the gluon distribution at small x and which are being measured at HERA. The observables are $\partial F_2/\partial \ln Q^2$, $F_2^c(x, Q^2)$ and the W dependence of the cross section for high energy diffractive J/ψ photoproduction. As expected J/ψ photoproduction offers an especially sensitive measure of the gluon.

Of course, these comparisons with data should be regarded as exploratory. To obtain a true quantitative prediction for all x we must include a proper treatment of the $z = 1$ behaviour and include the quark distributions in the evolution equation. Strictly we should also include the effects of energy-momentum conservation and even possible gluon shadowing corrections. The latter, however, are expected to be small in the HERA regime, as evidenced by the persistent rise of the F_2 data with decreasing x for Q^2 as low as $Q^2 = 2$ GeV^2. Last, but not least, the full next-to-leading $\ln(1/x)$ contribution is not understood at present. This is needed to check the prescription for the running of α_S and to specify the scale dependence.

My congratulations to the organisers for a very enjoyable Epiphany Conference. I would like to thank Professors A.D. Martin and J. Kwieciński for their collaboration in the work discussed here.

REFERENCES

[1] Yu.L. Dokshitzer, *Sov. Phys. JETP* **46**, 641 (1977); V. Gribov, L.N. Lipatov, *Sov. J. Nucl. Phys.* **15**, 78 (1972); L.N. Lipatov, *Sov. Phys. JETP* **20**, 181 (1974); G. Altarelli, G. Parisi, *Nucl. Phys.* **B126**, 298 (1977).

[2] E.A. Kuraev, L.N. Lipatov, V. Fadin, *Zh. Eksp. Teor. Fiz.* **72**, 373 (1977) (*Sov. Phys. JETP* **45**, 199 (1977)); Ya.Ya. Balitzkij, L.N. Lipatov, *Yad. Fiz.* **28**, 1597 (1978) (*Sov. J. Nucl. Phys.* **28**, 822 (1978)); L.N. Lipatov, in *Perturbative QCD*, edited by A.H. Mueller, World Scientific, Singapore 1989, p. 441; J.B. Bronzan, R.L. Sugar, *Phys. Rev.* **D17**, 585 (1978); T. Jaroszewicz, *Acta. Phys. Pol.* **B11**, 965 (1980).

[3] M. Ciafaloni, *Nucl. Phys.* **B296**, 49 (1988).

[4] S. Catani, F. Fiorani, G. Marchesini, *Phys. Lett.* **B234**, 339 (1990); *Nucl. Phys.* **B336**, 18 (1990); G. Marchesini, in Proceedings of the Workshop "QCD at 200 TeV", Erice, Italy, 1990, edited by L. Cifarelli and Yu.L. Dokshitzer, Plenum Press, New York, 1992, p.183; G. Marchesini, *Nucl. Phys.* **B445**, 49 (1995).
[5] J. Kwieciński, A.D. Martin, P.J. Sutton, *Phys. Rev.* **D52**, 1445 (1995).
[6] S. Catani, M. Ciafaloni, F. Hautmann, *Phys. Lett.* **B242**, 97 (1990); *Nucl. Phys.* **B366**, 657 (1991); J.C. Collins, R.K. Ellis, *Nucl. Phys.* **B360**, 3 (1991); E.M. Levin, M.G. Ryskin, A.G. Shuvaev, *Sov. J. Nucl. Phys.* **53**, 657 (1991).
[7] S. Catani, F. Hautmann, *Nucl. Phys.* **B427**, 475 (1994).
[8] A.J. Askew, J. Kwieciński, A.D. Martin, P.J. Sutton, *Phys. Rev.* **D47**, 3775 (1993).
[9] H1 collaboration: J. Dainton, Proc. of the Workshop on DIS and QCD, eds. J.F. Laporte and Y. Sirois, École Polytechnique, 1995 p. 37.
[10] ZEUS collaboration: B. Foster, Proc. of the Workshop on DIS and QCD, eds. J.F. Laporte and Y. Sirois, École Polytechnique, 1995) p. 57; ZEUS collaboration: M. Derrick *et al.*, DESY preprint 95-193, hep-ex/9510009.
[11] A.D. Martin, R.G. Roberts, W.J. Stirling, *Phys. Rev.* **D50**, 6734 (1994).
[12] A.D. Martin, R.G. Roberts, W.J. Stirling, *Phys. Lett.* **B354**, 155 (1995).
[13] B. Andersson, G. Gustafson, J. Samuelsson, Lund preprint LU TP 95-13.
[14] A.D. Martin, J. Kwiecinski, P.J. Sutton, Durham preprint DTP/96/02, hep-ph/9602320, to be published in *Z. Phys. C.*
[15] J.R. Forshaw, P.N. Harriman, P.J. Sutton, *Nucl. Phys.* **B416**, 739 (1994).
[16] H1 collaboration : A. De Roeck, these proceedings.
[17] EM Collaboration: J.J. Aubert *et al.*, *Nucl. Phys.* **B213**, 31 (1983).
[18] M. Glück, E. Reya, A. Vogt, *Z. Phys.* **C67**, 433 (1995).
[19] A. Vogt, DESY preprint DESY-96-012, hep-ph/9601352.
[20] J. Kwieciński, A.D. Martin, P.J. Sutton, Durham preprint DTP/95/94, hep-ph/9511263, to be published in *Phys. Rev. D.*
[21] M.G. Ryskin, R.G. Roberts, A.,D. Martin E.M. Levin, University of Durham report DTP/95/96.
[22] ZEUS collaboration: M. Derrick *et al.*, *Phys. Lett.* **B350**, 120 (1995); ZEUS and H1 collaborations; preliminary 1994 data presented at the Durham Workshop on HERA Physics, Sept. 1995, to be published.